

An integral-like numerical approach for solving Burgers' equation

Somrath Kanoksirirath^{a,*}

^a*NSTDA Supercomputer Center (ThaiSC), National Science and Technology Development Agency (NSTDA), Pathum Thani, 12120, Thailand*

Abstract

An integral-like approach established on spline polynomial interpolations is applied to the one-dimensional Burgers' equation. The Hopf-Cole transformation that converts non-linear Burgers' equation to linear diffusion problem is emulated by using Taylor series expansion. The diffusion equation is then solved by using analytic integral formulas. Four experiments were performed to examine its accuracy, stability and parallel scalability. The correctness of the numerical solutions is evaluated by comparing with exact solution and assessed error norms. Due to its integral-like characteristic, large time step can be employed without loss of accuracy and numerical stability. For practical applications, at least cubic interpolation is recommended. Parallel efficiency seen in the weak-scaling experiment depends on time step size but generally adequate.

Keywords: Burgers' equation, Integral-like approach, Hopf-Cole transformation, Explicit scheme
2000 MSC: 35Q35,

1. Introduction

The partial differential equation (PDE) of the form

$$\frac{\partial u}{\partial t} + u \frac{\partial u}{\partial x} = \nu \frac{\partial^2 u}{\partial x^2} \quad (1.1)$$

*Corresponding author.

Email address: somrath.kan@ncr.nstda.or.th (Somrath Kanoksirirath)

is called one-dimensional (1D) Burgers' equation. It models physical transport phenomena in fluid flows, turbulence, traffic flows and others. It is a vital part of Navier-Stokes equations where, in this case, u is a velocity of fluid and ν is a positive viscosity/diffusivity constant. The equation is a core of computational fluid dynamics, weather models, ocean models and hydrodynamic models.

The second term, uu_x , is non-linear. It hinders the development of a simple, stable and accurate numerical method for solving the Burgers' equation. Highly complex schemes usually have poor parallel scalability restricting its practicality up to a moderate-size problem. Similarly, severe stability condition restricts the time step size, leading to a high computational cost that unfavorable for some applications such as numerical weather prediction.

Although the solution of Burgers' equation can be obtained analytically by converting it to a diffusion equation, $\phi_t = \nu\phi_{xx}$, via using Hopf-Cole transform, Eq. (1.2)-(1.3), and then getting solved by applying Fourier transform or other approaches. It is inconvenient and unsuitable for arbitrary initial and boundary conditions normally presented in practice. Therefore, several numerical schemes have been developed.

$$\phi(x, t) = \exp\left(\frac{-1}{2\nu} \int_0^x u(\xi, t) d\xi\right) \quad (1.2)$$

$$u = -2\nu \frac{\phi_x}{\phi} \quad (1.3)$$

The standard numerical approach to tackle the non-linear term is to linearize it by assuming u in uu_x is locally constant [1, 2, 3, 4]. It can also be rewritten as $(u^2)_x$ then solved it accordingly [5]. On the other hand, Kutluay et al. [6] and Mukundan and Awasthi [7] developed a numerical Hopf-Cole transformation and solved the diffusion equation instead.

Regarding the numerical procedures, the finite element method is widely employed [1, 8, 9, 10, 11] as well as the Galerkin approach with a cubic polynomial as basis function [3, 6, 12, 13, 14]. Nevertheless, some used the conventional finite difference method [4, 7, 15]. Apart from grid-based schemes, Gao et al. [16] applied a particle-based scheme to the Burgers' equation. To speed up the implementation, Kumar et al. [17] developed a hybrid predictor-corrector scheme, while an artificial neural network is adopted to accelerated a prior Galerkin approach in [18].

In this paper, we introduce an integral-like approach that imitates mathematical transform and temporal integration to advance numerical solution

in time. Instead of the customary finite discretization, a spline interpolation is employed to represent gridded data as continuous functions. The general idea of this approach is explained in Section 2. In Section 3, the time-stepping method used in solving the diffusion equation is described as an example and as an indispensable part of the scheme for solving Burgers' equation. In Section 4, the numerical Hopf-Cole transformation is explained and the whole scheme is composed with additional remarks on programming aspect. In Section 5, the results of several numerical experiments are shown. Conclusions are made in Section 6.

2. Integral-like approach

The proposed integral-like approach is different from conventional methods in both numerical differentiation in space and numerical forwarding scheme in time. To solve a PDE, our data grid not only contains the necessary field variables but also their derivatives, so that the variables can be represented as a continuous function, found by applying a spline polynomial interpolation on any two adjacent grid points. To forward the variables in time, mathematical procedures along with additional approximations, according to the corresponding analytical solution, are emulated by using the known continuous spline polynomial function. The derivatives are also needed to be updated in time. Nevertheless, initializing the derivatives by using a finite difference scheme is sufficient. Because we can split terms in a PDE and solve more but simpler PDEs, the requirement of analytical solution is not too restrict. For example, the advection-diffusion equation $\phi_t + \alpha\phi_x = \nu\phi_{xx}$ can be splitted into two stages, i.e., advection $\phi_t + \alpha\phi_x = 0$ and diffusion $\phi_t = \nu\phi_{xx}$, then solved numerically. A simple case is demonstrated later in Example 4, while more complicated models are discussed in [19].

In this paper, integral-like methods utilizing linear, cubic and quintic spline interpolations are investigated. They will be referred as linear grid scheme (LG), cubic grid scheme (CG) and quintic grid scheme (QG) respectively. More details are provided in Table 1. For cubic and quintic schemes, the second-order central finite difference is used to initialize u_x and u_{xx} except at the two end points where the first-order forward and backward finite difference are used instead.

To forward the numerical solution of the Burgers' equation in time, Hopf-Cole transformation is applied numerically, the resulting diffusion equation is solved in the Hopf-Cole space and then converted back to normal space.

Scheme	Local spline polynomial $P_j(y)$	Data grid
Linear (LG)	$a_j y + b_j$	u
Cubic (CG)	$a_j y^3 + b_j y^2 + c_j y + d_j$	u
	$3a_j y^2 + 2b_j y + c_j$	u_x
Quintic (QG)	$a_j y^5 + b_j y^4 + c_j y^3 + d_j y^2 + e_j y + f_j$	u
	$5a_j y^4 + 4b_j y^3 + 3c_j y^2 + 2d_j y + e_j$	u_x
	$20a_j y^3 + 12b_j y^2 + 6c_j y + 2d_j$	u_{xx}

Table 1: Integral-like schemes with their associated spline polynomial interpolations P_j for u, u_x and u_{xx} between x_j and x_{j+1} where $y = x - x_j$ and $0 \leq y < \Delta x$

In the following sections, these three steps are explained. However, how the integral-like approach can be applied to the diffusion equation is discussed first to familiarize readers with the general idea of the method. It is worth noting that the integral-like approach is an explicit scheme that incorporating mathematical formulas and it is equivalent to a Semi-Lagrangian method when applied to the linear advection equation.

3. Method for linear diffusion

The linear diffusion equation, $\phi_t = \nu \phi_{xx}$ where ν is a positive diffusion constant can be solved analytically using Fourier transform. This approach is derived in textbooks such as [20] and [21]. The resulting analytical solution is

$$\phi(x, t) = \int_{-\infty}^{\infty} \frac{1}{\sqrt{4\pi\nu t}} \exp\left(-\frac{(x-\xi)^2}{4\nu t}\right) \phi(\xi, 0) d\xi \quad (3.1)$$

with analytical boundary conditions $\phi(\infty, t) = \phi(-\infty, t) = 0$.

Time-stepping scheme of the integral-like approach can be derived from Eq. (3.1) by substituting the spline polynomial function $P_j(y, t)$ in and changing the time interval. In the case of the cubic scheme (CG) with n_x

equally-spacing grid points, Eq. (3.1) becomes

$$\begin{aligned}\phi(x_i, t + \Delta t) &= \sum_{j=-\infty}^{\infty} \int_0^{\Delta x} \frac{1}{\sqrt{4\pi\nu\Delta t}} \exp\left(-\frac{(x_i - (\xi_j + y))^2}{4\nu\Delta t}\right) P_j(y, t) d(\xi_j + y) \\ &\approx \frac{1}{\sqrt{4\pi\nu\Delta t}} \sum_{|\ell_{i,j}| \leq 5\sigma} \int_0^{\Delta x} \exp\left(-\frac{(y + \ell_{i,j})^2}{4\nu\Delta t}\right) (a_j y^3 + b_j y^2 + c_j y + d_j) dy\end{aligned}\tag{3.2}$$

Because of the Gaussian decay term, the summation range can be limited to j such that the relative distance $\ell_{i,j} \equiv \xi_j - x_i$ is within a margin; five standard deviation $5\sigma = 5\sqrt{2\nu\Delta t}$ is chosen for this paper.

Experimentally, it was found that all the three methods are numerically stable if the 5σ marginal range is larger than the grid spacing Δx . This is equivalent to $d \geq 0.02$ where $d = \nu(\Delta t)/(\Delta x)^2$ is non-dimensional diffusion number. Unmistakeably, the sign is reversed of what normally found for finite difference schemes. Because the 5σ length is an estimation, the obtained stability condition $d \geq 0.02$, therefore, is not absolute. Generally, we found that the higher, the order of the spline polynomial is used, the larger, the diffusion number is required.

Due to the summation of j within the marginal range, time complexity of the integral-like methods is $\mathcal{O}((5\sigma/\Delta x) n_x n_t) \sim \mathcal{O}((\sqrt{\nu\Delta t}/\Delta x) n_x n_t) \sim \mathcal{O}(\sqrt{\nu} n_x^2 n_t^{1/2})$ where n_x is the number of grid points and n_t is the total number of time step.

Another implication of the marginal range is that the boundary conditions may have to be specified by a small set of points, instead of a single point exactly at the boundary. In the case of periodic boundary condition, the required outside point $-j$ on the left of the considered domain is corresponding to the inside point $n - j$. Likewise, the values at the outside point $n_x + j$ on the right are that of the j point. For Dirichlet and no-flux boundary conditions, reflected points or their mirror images could be used. Adding additional points to both ends can keep the implementation simple and is adopted here as it also matches with the domain decomposition method for parallelization.

In Eq. (3.2), the indefinite integral of the form, $\int y^m \exp(-(y + \ell)^2/\delta) dy$ where m is a positive integer, is evaluated recursively using Eqs. (3.3) - (3.5),

which derived by applying integration by parts.

$$\begin{aligned}
PG_m &\equiv \int y^m \exp\left(-\frac{(y+\ell)^2}{\delta}\right) dy \\
&= (m-1) \frac{\delta}{2} PG_{m-2} - \ell PG_{m-1} - \frac{\delta}{2} y^{m-1} \exp\left(-\frac{(y-\ell)^2}{\delta}\right) \quad (3.3)
\end{aligned}$$

where

$$PG_0 = \frac{\sqrt{\pi\delta}}{2} \left[\operatorname{erf}\left(\frac{y+\ell}{\sqrt{\delta}}\right) - \operatorname{erf}\left(\frac{\ell}{\sqrt{\delta}}\right) \right] \quad (3.4)$$

$$PG_1 = -\frac{\ell\sqrt{\pi\delta}}{2} \left[\operatorname{erf}\left(\frac{y+\ell}{\sqrt{\delta}}\right) - \operatorname{erf}\left(\frac{\ell}{\sqrt{\delta}}\right) \right] - \frac{\delta}{2} \left[\exp\left(-\frac{(y+\ell)^2}{\delta}\right) - \exp\left(-\frac{\ell^2}{\delta}\right) \right] \quad (3.5)$$

On the other hand, the coefficients of the cubic spline polynomial function $P_j(y)$, i.e., a_j, b_j, c_j and d_j , are found by solving Eqs. (3.6) - (3.9) at each time step—they are analytically solved beforehand to speed up our implementation.

$$P_j(\Delta x, t) = \phi_{j+1} = a_j(\Delta x)^3 + b_j(\Delta x)^2 + c_j(\Delta x) + d_j \quad (3.6)$$

$$\partial_x P_j(\Delta x, t) = \partial_x \phi_{j+1} = 3a_j(\Delta x)^2 + 2b_j(\Delta x) + c_j \quad (3.7)$$

$$P_j(0, t) = \phi_j = d_j \quad (3.8)$$

$$\partial_x P_j(0, t) = \partial_x \phi_j = c_j \quad (3.9)$$

We denote that $\partial_x \phi_j$ represents the first derivative of ϕ at grid point j . The derivatives are stored in a data grid and are updated by using Eq. (3.10),

which derived by differentiating Eq. (3.2) with respect to x_i .

$$\begin{aligned}
\frac{\partial}{\partial x_i} \phi(x_i, t + \Delta t) &= \frac{1}{\sqrt{4\pi\nu\Delta t}} \sum_{|\ell_{i,j}| \leq 5\sigma} \int_0^{\Delta x} \left[\frac{\partial(\xi_j - x_i)}{\partial x_i} \frac{\partial}{\partial \ell_{i,j}} \exp\left(-\frac{(y + \ell_{i,j})^2}{4\nu\Delta t}\right) \right] \\
&\quad \left(a_j y^3 + b_j y^2 + c_j y + d_j \right) dy \\
&= \frac{1}{\sqrt{4\pi\nu\Delta t}} \sum_{|\ell_{i,j}| \leq 5\sigma} \int_0^{\Delta x} \left[(-1) \left(\frac{-2(y + \ell_{i,j})}{4\nu\Delta t} \right) \exp\left(-\frac{(y + \ell_{i,j})^2}{4\nu\Delta t}\right) \right] \\
&\quad \left(a_j y^3 + b_j y^2 + c_j y + d_j \right) dy \\
&= \frac{1}{(2\nu\Delta t)\sqrt{4\pi\nu\Delta t}} \sum_{|\ell_{i,j}| \leq 5\sigma} \int_0^{\Delta x} \exp\left(-\frac{(y + \ell_{i,j})^2}{4\nu\Delta t}\right) \\
&\quad \left(a_j y^4 + (b_j + \ell_{i,j} a_j) y^3 + (c_j + \ell_{i,j} b_j) y^2 + (d_j + \ell_{i,j} c_j) y + \ell_{i,j} d_j \right) dy
\end{aligned} \tag{3.10}$$

Hence, Eqs. (3.2) and (3.10) together form the complete time-stepping method for the integral-like cubic scheme. Their computation are abetted by Eqs. (3.3) - (3.9). The derivation of the linear scheme and the quintic scheme are as of the cubic scheme but with different form of spline polynomial $P_j(y)$ substituting in and with different number of data grid to be stored and iterated in time.

4. Method for Hopf-Cole transformation

To the best of our knowledge, [15] and [7] are the pioneers who employed the Hopf-Cole transformation in numerical scheme for solving Burgers' equation. They portrays the transformation through an infinite series, while solving the diffusion equation by using a finite difference method; their implementation, therefore, is different from ours.

For our cubic scheme, the first step in performing Hopf-Cole transformation from u to ϕ , i.e., Eq. (1.2), is to compute the integral of u as in Eq.

(4.1).

$$\begin{aligned}
\text{Int}(u) &\equiv \int_{0'}^{x_i} u(\xi, t) d\xi = \sum_{j=0}^{i-1} \int_0^{\Delta x} P_j(\xi, t) d\xi \\
&= \sum_{j=0}^{i-1} \int_0^{\Delta x} \left(a_j \xi^3 + b_j \xi^2 + c_j \xi + d_j \right) d\xi \\
&= \sum_{j=0}^{i-1} a_j \frac{(\Delta x)^4}{4} + b_j \frac{(\Delta x)^3}{3} + c_j \frac{(\Delta x)^2}{2} + d_j (\Delta x)
\end{aligned} \tag{4.1}$$

Then, the exponent $-(1/2\nu)\text{Int}(u)$ in Eq. (1.2) is represented as a quintic spline polynomial function by using $\text{Int}(u)$, u and u_x . The quintic coefficients are found by solving six linear equations developed analogously as Eqs. (3.6) - (3.9).

Then, for a quintic polynomial Q_i of the i segment, the value of ϕ between x_i and x_{i+1} are written as a Taylor series T_i of $\exp(Q_i)$. In our implementation, the number of terms are varied adaptively to ensure that the deviation of T_i is less than 0.01%. The resulting ϕ or T_i , which satisfying the diffusion equation, is then solved by the method discussed in Section 3.

On the other hand, the Hopf-Cole transformation from ϕ to u in Eq. (1.3) is done by direct substitution. For example, u and u_x of the cubic scheme is deduced from ϕ , ϕ_x and ϕ_{xx} by using Eqs. (4.2) and (4.3).

$$u_i = -2\nu \left(\frac{\partial_x \phi_i}{\phi_i} \right) \tag{4.2}$$

$$\partial_x u_i = -2\nu \left(\frac{\phi_i (\partial_x^2 \phi_i) - (\partial_x \phi_i)^2}{\phi_i^2} \right) \tag{4.3}$$

To sum up, an integral-like scheme for solving Burgers' equation mainly consists of (1) Numerical Hopf-Cole integration scheme for transforming from u space to ϕ space, (2) Numerical diffusion scheme for advancing $\phi(x, t)$ and its required derivatives to $t + \Delta t$, (3) Numerical Hopf-Cole differentiation scheme for transforming $\phi(x, t + \Delta t)$ and its derivatives back to u space, and (4) Spline interpolation method for representing discrete data points as a continuous function for the computation in (1)-(3). One complete time iteration step Δt for solving Burgers' equation is composed of (1), (2) and

(3). Supplementarily, as mentioned, finite difference scheme is employed for computing the initial derivatives such as $u_x(x, t_0)$ from $u(x, t_0)$.

Because the numerical Hopf-Cole integration step involves rapid exponential decay/growth, when implementing in a computer language, at least double-precision floating-point data type is recommended. Numerical round-off error must be carefully minimized. Moreover, additional memory allocation is required for the derivatives of the cubic scheme and the quintic scheme, resulting in space complexity of $\mathcal{O}(4n_x)$ and $\mathcal{O}(6n_x)$ respectively. The common factor of 2 is because a temporary array is needed for keeping updated value at each position, before entirely transferred to the primary array in the final step. For our current implementation, another n_x array is used to store $\text{Int}(u)$.

The benefit of adaptive grid was also explored. Our implementation redistributes grid points according to path length of u , accurately approximated by Gaussian quadrature. However, the numerical solution appears to be less accurate due to numerical error introduced when repeatedly rearranging the grids. Therefore, our unsuccessful implementation of the adaptive grid is not discussed in this paper, but shortly noted. This is to inform the possibility that adaptive grid may not be able to improve integral-like schemes in general.

5. Numerical experiment

In this section, four test cases are used to evaluate the integral-like methods in Table 1. Accuracy and parallel scalability are considered in Example 1-3. In Example 4, the viability of the split approach, for applying the integral-like method to more complicated problems than 1D Burgers' equation, is investigated.

To quantify the accuracy of the schemes when comparing with exact/analytical solutions $f(x)$, l_1 , l_2 and l_∞ error norm are adopted. Their definitions for

equally-spacing grid are

$$\ell_1(u) = \frac{\sum_{j=0}^n |u_j - f(x_j)|}{\sum_{j=0}^n |f(x_j)|} \quad (5.1)$$

$$\ell_2(u) = \frac{\sqrt{\sum_{j=0}^n (u_j - f(x_j))^2}}{\sqrt{\sum_{j=0}^n f(x_j)^2}} \quad (5.2)$$

$$\ell_\infty(u) = \frac{\max |u_j - f(x_j)|}{\max |f(x_j)|} \quad (5.3)$$

Example 1. Burgers' equation (Eq. 1.1) with the Dirichlet boundary condition

$$u(0, t) = u(1.2, t) = 0 \quad (5.4)$$

and the analytical solution

$$u(x, t) = \frac{x/t}{1 + \sqrt{t/t_0} \exp(x^2/4\nu t)} \quad (5.5)$$

where $t \geq 1$ and $t_0 = \exp(0.125/\nu)$ are considered as in [16], [22] and [23]. The solution and the corresponding numerical results are shown in Fig. 1, using $\nu = 0.005$, $\Delta x = 0.02$ and $\Delta t = 0.02$.

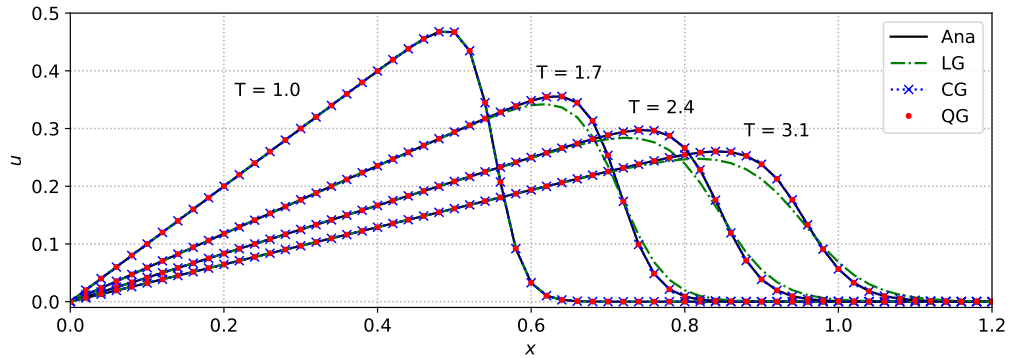


Figure 1: Numerical solutions and analytical solution of Example 1: $\nu = 0.005$, $\Delta x = 0.02$ and $\Delta t = 0.02$

Numerical values and exact solution for $\nu = 0.005$ and $\Delta t = 0.02$ at $t = 2.4$ are given in Table 2, using $\Delta x = 0.02$ and 0.01 . The numerical results

Position	Δx	LG	CG	QG	Exact
0.1	0.02	0.041664	0.041762	0.041799	0.041667
	0.01	0.041665	0.041690	0.041694	
0.2	0.02	0.083328	0.083375	0.083390	0.083333
	0.01	0.083331	0.083343	0.083344	
0.3	0.02	0.124995	0.125015	0.125018	0.125000
	0.01	0.124996	0.125001	0.125001	
0.4	0.02	0.166648	0.166666	0.166663	0.166665
	0.01	0.166659	0.166661	0.166661	
0.5	0.02	0.208207	0.208313	0.208307	0.208318
	0.01	0.208299	0.208311	0.208310	
0.6	0.02	0.248953	0.249809	0.249798	0.249816
	0.01	0.249681	0.249806	0.249804	
0.7	0.02	0.281531	0.288475	0.288445	0.288472
	0.01	0.287090	0.288458	0.288454	
0.8	0.02	0.239172	0.266132	0.266155	0.266228
	0.01	0.258598	0.266184	0.266179	
0.9	0.02	0.055092	0.038663	0.038622	0.038651
	0.01	0.043197	0.038638	0.038633	

Table 2: Numerical results and exact solution of Example 1 at $t = 2.4$ using $\nu = 0.005$ and $\Delta t = 0.02$

Scheme	Δx	Δt	d	ℓ_1	ℓ_2	ℓ_∞
LG	0.02	0.035	0.4375	1.77e-02	2.86e-02	5.55e-02
	0.02	0.020	0.2500	3.09e-02	4.85e-02	9.10e-02
	0.01	0.020	1.0000	7.82e-03	1.30e-02	2.56e-02
	0.01	0.005	0.2500	3.12e-02	4.91e-02	9.18e-02
CG	0.02	0.035	0.4375	3.79e-04	4.45e-04	8.24e-04
	0.02	0.020	0.2500	2.34e-04	3.00e-04	4.78e-04
	0.01	0.020	1.0000	9.99e-05	1.12e-04	1.77e-04
	0.01	0.005	0.2500	2.16e-04	2.33e-04	3.86e-04
QG	0.02	0.035	0.4375	5.49e-04	6.30e-04	1.01e-03
	0.02	0.020	0.2500	3.29e-04	4.02e-04	6.84e-04
	0.01	0.020	1.0000	1.20e-04	1.33e-04	2.01e-04
	0.01	0.005	0.2500	3.68e-04	3.99e-04	6.41e-04

Table 3: Error norms of Example 1 at $t = 2.4$, using $\nu = 0.005$.

and the exact solution are in a good agreement. In Table 3, the error norms are computed for four different pairs of Δx and Δt . From the results, the linear scheme (LG) performs the worst, while the cubic scheme (CG) seem to be slightly better than the quintic scheme (QG). For CG and QG, as the grid spacing and time step size are reduced, the error norms decrease. However, too small time step size appears to introduce more numerical errors. This may be from the procedure in Eq. (3.4) and (3.5) where smaller $\delta = 4\nu \Delta t$ could lead to bigger round-off error—and possibly because the methods are not discrete but continuous integral-like.

Example 2. Burgers' equation (Eq. 1.1) with the initial condition

$$u(x, 0) = \sin(\pi x) \quad (5.6)$$

and the analytical solution

$$u(x, t) = \frac{4\pi\nu \sum_{k=1}^{\infty} k A_k \sin(k\pi x) \exp(-k^2\pi^2\nu t)}{A_0 + 2 \sum_{k=1}^{\infty} A_k \cos(k\pi x) \exp(-k^2\pi^2\nu t)} \quad (5.7)$$

where

$$A_k = \int_0^1 \cos(k\pi x) \exp\left(\frac{\cos(\pi x) - 1}{2\pi\nu}\right) dx \quad (5.8)$$

are considered. Unlike in [16] and [22], periodic boundary condition is applied for $0 \leq x \leq 1$, $\nu = 0.01$, $\Delta x = 0.02$, and $\Delta t = 0.005$. The results are plotted in Fig. 2.

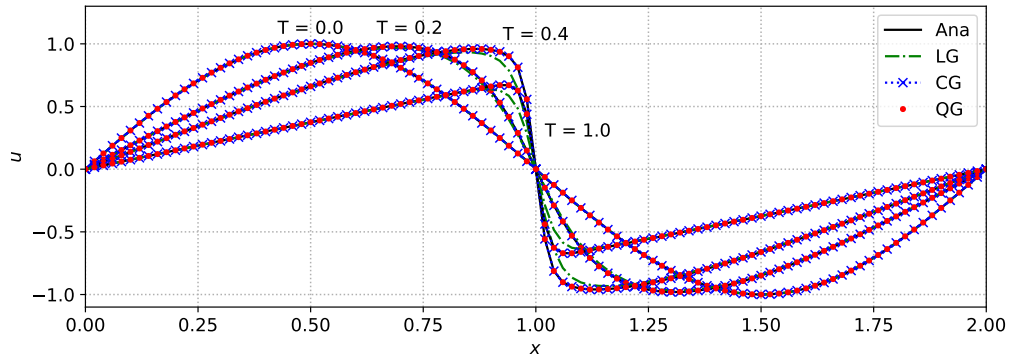


Figure 2: Numerical solutions and analytical solution of Example 2: $\nu = 0.01$, $\Delta x = 0.02$, and $\Delta t = 0.005$

Position	Δx	LG	CG	QG	Exact
0.1	0.02	0.065558	0.066306	0.066305	0.066316
	0.01	0.066101	0.066284	0.066283	
0.2	0.02	0.129578	0.131189	0.131187	0.131209
	0.01	0.130750	0.131145	0.131144	
0.3	0.02	0.190039	0.192755	0.192752	0.192786
	0.01	0.192020	0.192689	0.192687	
0.4	0.02	0.243809	0.247999	0.247995	0.248041
	0.01	0.246874	0.247910	0.247908	
0.5	0.02	0.285749	0.291864	0.291859	0.291916
	0.01	0.290232	0.291752	0.291749	
0.6	0.02	0.307656	0.316005	0.316000	0.316068
	0.01	0.313784	0.315876	0.315872	
0.7	0.02	0.297804	0.308022	0.308017	0.308089
	0.01	0.305304	0.307884	0.307880	
0.8	0.02	0.243417	0.253657	0.253653	0.253718
	0.01	0.250927	0.253533	0.253529	
0.9	0.02	0.139279	0.146027	0.146025	0.146065
	0.01	0.144223	0.145951	0.145949	

Table 4: Numerical results and exact solution of Example 2 at $t = 1.0$ using $\nu = 0.1$ and $\Delta t = 0.01$

Scheme	Δx	Δt	d	ℓ_1	ℓ_2	ℓ_∞
LG	0.02	0.0200	5.0	1.35e-02	1.46e-02	1.72e-02
	0.02	0.0100	2.5	2.64e-02	2.85e-02	3.35e-02
	0.01	0.0100	10.0	7.19e-03	7.75e-03	9.07e-03
	0.01	0.0025	2.5	2.70e-02	2.92e-02	3.42e-02
CG	0.02	0.0200	5.0	4.25e-04	4.33e-04	4.56e-04
	0.02	0.0100	2.5	1.97e-04	2.00e-04	2.11e-04
	0.01	0.0100	10.0	6.07e-04	6.16e-04	6.46e-04
	0.01	0.0025	2.5	8.27e-04	8.39e-04	8.76e-04
QG	0.02	0.0200	5.0	4.40e-04	4.48e-04	4.72e-04
	0.02	0.0100	2.5	2.12e-04	2.15e-04	2.26e-04
	0.01	0.0100	10.0	6.18e-04	6.28e-04	6.58e-04
	0.01	0.0025	2.5	8.97e-04	9.10e-04	9.50e-04

Table 5: Error norms of Example 2 at $t = 1.0$ using $\nu = 0.1$.

Numerical results, exact solution and error norms at $t = 1$ are presented in Table 4 and 5. Similar features can be seen as in Example 1. Therefore, although the quintic scheme employs a higher-order spline interpolation method, it is currently worse than the cubic scheme. This may be caused by numerical round-off errors that could be diminished when higher-precision data type is used. As the accuracy cannot be further improved with smaller Δt and/or Δx , it is evident that these integral-like schemes are susceptible to round-off errors.

Example 3. Burgers' equation (Eq. 1.1) with step initial condition at $x = 0$ is employed to study the parallel scalability of the integral-like methods. The analytical solution for infinite boundary conditions $u(-\infty, t) = 1$ and $u(\infty, t) = 0$ is

$$u(x, t) = \frac{\operatorname{erfc}\left(\frac{x-t}{2\sqrt{\nu t}}\right)}{\operatorname{erfc}\left(-\frac{x}{2\sqrt{\nu t}}\right) \exp\left(\frac{x-t/2}{2\nu}\right) + \operatorname{erfc}\left(\frac{x-t}{2\sqrt{\nu t}}\right)} \quad (5.9)$$

which becomes a traveling-wave solution thereafter about $t = 10$. The numerical results are shown in Fig. 3 for $\nu = 1$, $\Delta x = 0.6$ and $\Delta t = 0.04$. The result of the linear scheme (LG) is significantly worse than the other two.

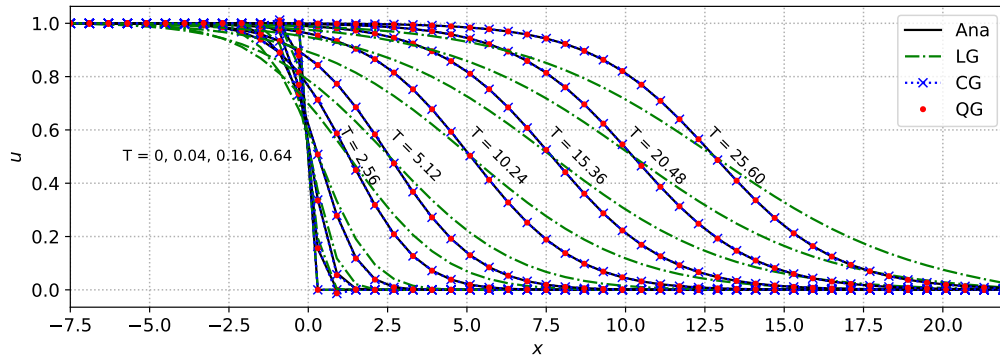


Figure 3: Numerical solutions and analytical solution of Example 3: $\nu = 1$, $\Delta x = 0.6$ and $\Delta t = 0.04$

To test parallel efficiency of the integral-like methods, a weak-scaling experiment was performed using TARA cluster at NSTDA supercomputer center (ThaiSC). Both number of grid point and number of time step are adjusted to scale computation workload, while having grid spacing Δx and

the marginal range $5\sigma = 5\sqrt{2\nu\Delta t}$ approximately unaltered, that is, while having roughly the same number of $u(x_j, t)$ used in updating $u(x_i, t + \Delta t)$.

With N_s representing a running variable, the number of employed CPU core is $N_{\text{core}} = N_s^2$ operating on the total number of grid point $n_x = 500 N_s + 1$ for domain $[-15, 400 N_s + 20]$ simulating from $t_0 = 10$ to $t = 800 N_s + 10$. The time step size Δt is varied to explore how parallel scalability is affected by the marginal range 5σ , because the bigger the marginal range is, the larger the overlapped areas of the domain decomposition algorithm are.

Utilized compute nodes of TARA cluster are equipped with two Intel Xeon Gold 6148 CPU (2.40GHz) with the hyper-threading technology disabled. A TARA compute node has totally 40 CPU cores and 192GB of RAM. On the other hand, our program was coded in Python3 and parallelized using mpi4py library, before getting ported to C through Cython and compiled on TARA using foss-2021b toolchain.

The weak-scaling parallel efficiency $R(1)/R(N_s)$, where $R(N_s)$ is wall-clock runtime of the N_s scaled case, is plotted in Fig. 4 from $N_s = 1$ to $N_s = 10$. The N_s scaled case is executed using N_s^2 CPU cores. The serial runtime $R(1)$ of each scheme is given in Table 6.

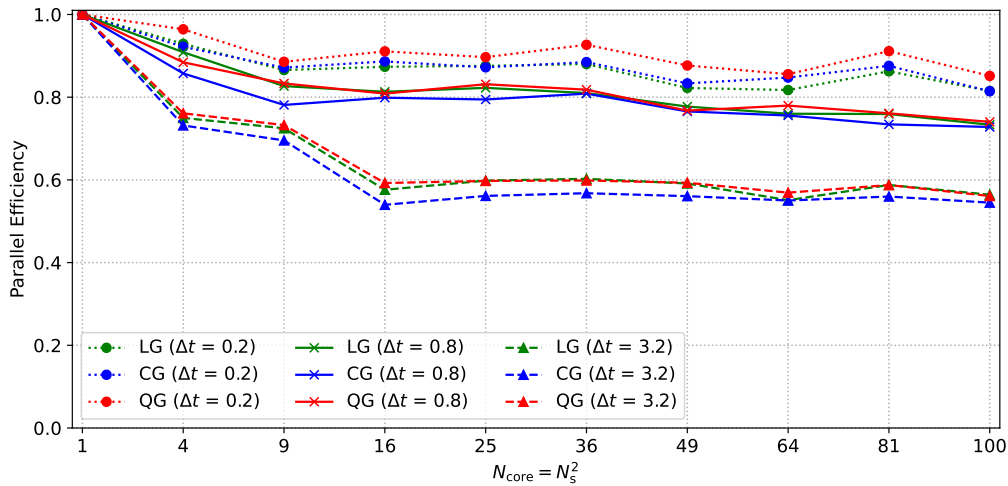


Figure 4: Weak-scaling parallel efficiency of the integral-like schemes for Burgers' equation using time step size $\Delta t = 0.2, 0.8$ and 3.2 .

According to Fig. 4, the parallel efficiency of the integral-like schemes decreases as larger time step size Δt is chosen. However, from Table 6, the

Δt	5σ	d	Runtime (sec)		
			LG	CG	QG
0.2	3.16	0.26-0.31	1,944.50	3,170.80	4,713.98
0.8	6.32	1.05-1.23	889.65	1,420.01	2,069.45
3.2	12.65	4.22-4.92	327.19	507.69	756.70

Table 6: The wall-clock serial runtime $R(1)$ of each integral-like scheme for different time step size Δt , but ran for the same simulation time, i.e., from $t_0 = 10$ to $t = 810$.

wall-clock runtime of larger time step size is evidently lower. Therefore, time step size of operational applications may have be varied according to available resources. The parallel efficiency also declines as the problem size becomes larger and more CPU cores are used, but reduces significantly slower when the number of CPU cores is more than ten.

Example 4. Burgers' equation with additional source term

$$\frac{\partial u}{\partial t} + u \frac{\partial u}{\partial x} = \nu \frac{\partial^2 u}{\partial x^2} - 3u(1-u)(1-2u) \quad (5.10)$$

is considered to illustrate the split approach, which separate terms in the equation into stages and successively solve them for an iteration. Applying the split approach to Eq. (5.10), the stage equations are

$$\frac{\partial u}{\partial t} + u \frac{\partial u}{\partial x} = \nu \frac{\partial^2 u}{\partial x^2} \quad (5.11)$$

$$\frac{\partial u}{\partial t} = -3u(1-u)(1-2u) \quad (5.12)$$

The first stage, i.e., Eq. (5.11), is the Burger's equation; therefore, the schemes explained in prior sections can be readily applied. The second stage, i.e, Eq. (5.12), is a growth/decay equation with analytical solution found by solving

$$A e^{-3t} = \frac{1}{4} - \frac{1}{4(2u-1)^2}$$

Therefore, the integral-like scheme for Eq. (5.12) is

$$u(x_i, t + \Delta t) = \frac{1}{2} \left(1 \pm \frac{1}{\sqrt{1 - 4A \exp(-3\Delta t)}} \right)$$

where

$$A = \frac{1}{4} \left(1 - \frac{1}{(2u(x_i, t) - 1)^2} \right)$$

Following [24], an exact solution of Eq. (5.10) when $\nu = 1$ is

$$u(x, t) = \frac{1}{2} \left(1 - \tanh \left(x - \frac{t}{2} \right) \right) \quad (5.13)$$

Using the other parameters as for Fig. 3, the numerical results of CG and QG agree well with the analytical solution as seen in Fig. 5. Experimentally, the numerical solutions agree well with the exact solution when $\Delta t < 1$.

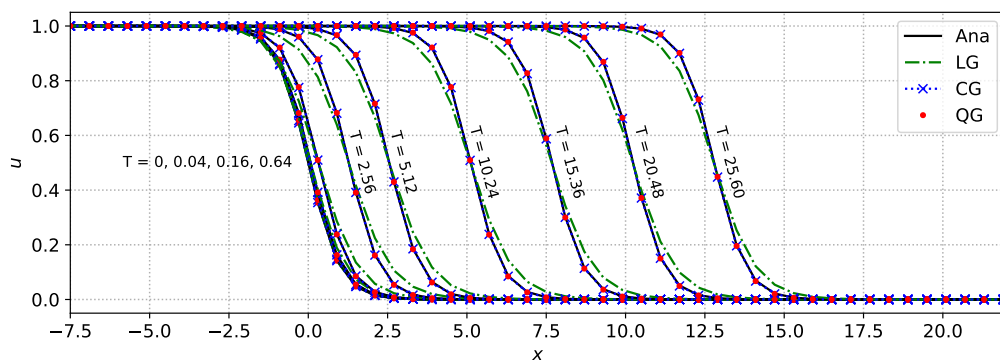


Figure 5: Numerical solutions and analytical solution of Example 4: $\nu = 1$, $\Delta x = 0.6$ and $\Delta t = 0.04$

6. Conclusions

In this study, a numerical approach based on continuous representation of variables by using local polynomial interpolation is explored. When applying to the one-dimensional Burgers' equation, the derived explicit schemes are numerically stable at large time step size Δt . Evaluated by four different test cases, the numerical results agree well with their corresponding exact solution when at least cubic interpolation is employed. The results indicate that the cubic scheme (CG) is the most efficient, having error norms of order 10^{-4} when time step size of around 0.01 is used. Although the weak-scaling parallel efficiency is generally good, it becomes worse as bigger time step size is chosen. Overall, it is a promising approach for applications that require a fast, stable and reliable method, such as numerical weather prediction.

Acknowledgments

I would like to thank NSTDA supercomputer center (ThaiSC) for their generous support in both time and computational resources.

References

- [1] A. Dogan, A galerkin finite element approach to burgers' equation, *Applied Mathematics and Computation* 157 (2) (2004) 331–346. doi:<https://doi.org/10.1016/j.amc.2003.08.037>.
- [2] Y. Hon, X. Mao, An efficient numerical scheme for burgers' equation, *Applied Mathematics and Computation* 95 (1) (1998) 37–50. doi:[https://doi.org/10.1016/S0096-3003\(97\)10060-1](https://doi.org/10.1016/S0096-3003(97)10060-1).
- [3] I. Ganaie, V. Kukreja, Numerical solution of burgers' equation by cubic hermite collocation method, *Applied Mathematics and Computation* 237 (2014) 571–581. doi:<https://doi.org/10.1016/j.amc.2014.03.102>.
- [4] X. Yang, Y. Ge, B. Lan, A class of compact finite difference schemes for solving the 2d and 3d burgers' equations, *Mathematics and Computers in Simulation* 185 (2021) 510–534. doi:<https://doi.org/10.1016/j.matcom.2021.01.009>.
- [5] Y. Guo, Y. feng Shi, Y. min Li, A fifth-order finite volume weighted compact scheme for solving one-dimensional burgers' equation, *Applied Mathematics and Computation* 281 (2016) 172–185. doi:<https://doi.org/10.1016/j.amc.2016.01.061>.
- [6] S. S. Kumbhar, S. Thakar, Galerkin finite element method for forced burgers' equation, *Journal of Mathematical Modeling* 7 (4) (2019) 445–467. doi:[10.22124/jmm.2019.13259.1265](https://doi.org/10.22124/jmm.2019.13259.1265).
- [7] V. Mukundan, A. Awasthi, Efficient numerical techniques for burgers' equation, *Applied Mathematics and Computation* 262 (2015) 282–297. doi:<https://doi.org/10.1016/j.amc.2015.03.122>.
- [8] J. Caldwell, P. Wanless, A. Cook, A finite element approach to burgers' equation, *Applied Mathematical Modelling* 5 (3) (1981) 189–193. doi:[https://doi.org/10.1016/0307-904X\(81\)90043-3](https://doi.org/10.1016/0307-904X(81)90043-3).

- [9] J. Caldwell, P. Smith, Solution of burgers' equation with a large reynolds number, *Applied Mathematical Modelling* 6 (5) (1982) 381–385. doi:[https://doi.org/10.1016/S0307-904X\(82\)80102-9](https://doi.org/10.1016/S0307-904X(82)80102-9).
- [10] E. Aksan, A numerical solution of burgers' equation by finite element method constructed on the method of discretization in time, *Applied Mathematics and Computation* 170 (2) (2005) 895–904. doi:<https://doi.org/10.1016/j.amc.2004.12.027>.
- [11] Y. Chai, J. Ouyang, Appropriate stabilized galerkin approaches for solving two-dimensional coupled burgers' equations at high reynolds numbers, *Computers & Mathematics with Applications* 79 (5) (2020) 1287–1301. doi:<https://doi.org/10.1016/j.camwa.2019.08.036>.
- [12] G. Arora, B. K. Singh, Numerical solution of burgers' equation with modified cubic b-spline differential quadrature method, *Applied Mathematics and Computation* 224 (2013) 166–177. doi:<https://doi.org/10.1016/j.amc.2013.08.071>.
- [13] M. Tamsir, N. Dhiman, V. K. Srivastava, Extended modified cubic b-spline algorithm for nonlinear burgers' equation, *Beni-Suef University Journal of Basic and Applied Sciences* 5 (3) (2016) 244–254. doi:<https://doi.org/10.1016/j.bjbas.2016.09.001>.
- [14] B. K. Singh, M. Gupta, A new efficient fourth order collocation scheme for solving burgers' equation, *Applied Mathematics and Computation* 399 (2021) 126011. doi:<https://doi.org/10.1016/j.amc.2021.126011>.
- [15] S. Kutluay, A. Bahadir, A. Özdeş, Numerical solution of one-dimensional burgers equation: explicit and exact-explicit finite difference methods, *Journal of Computational and Applied Mathematics* 103 (2) (1999) 251–261. doi:[https://doi.org/10.1016/S0377-0427\(98\)00261-1](https://doi.org/10.1016/S0377-0427(98)00261-1).
- [16] Y. Gao, L.-H. Le, B.-C. Shi, Numerical solution of burgers' equation by lattice boltzmann method, *Applied Mathematics and Computation* 219 (14) (2013) 7685–7692. doi:<https://doi.org/10.1016/j.amc.2013.01.056>.
- [17] N. Kumar, R. Majumdar, S. Singh, Predictor–corrector nodal integral method for simulation of high reynolds number fluid flow using larger

- time steps in burgers' equation, *Computers & Mathematics with Applications* 79 (5) (2020) 1362–1381. doi:<https://doi.org/10.1016/j.camwa.2019.09.001>.
- [18] F. M. de Lara, E. Ferrer, Accelerating high order discontinuous galerkin solvers using neural networks: 1d burgers' equation, *Computers & Fluids* 235 (2022) 105274. doi:<https://doi.org/10.1016/j.compfluid.2021.105274>.
- [19] R. Bridson, *Fluid Simulation for Computer Graphics*, Second Edition, Taylor & Francis, 2015.
- [20] M. Stone, P. Goldbart, *Mathematics for Physics: A Guided Tour for Graduate Students*, Cambridge University Press, 2009.
- [21] P. Olver, *Introduction to Partial Differential Equations*, Undergraduate Texts in Mathematics, Springer International Publishing, 2013.
- [22] M. Sarboland, A. Aminataei, On the numerical solution of one-dimensional nonlinear nonhomogeneous burgers' equation, *J. Appl. Math.* 2014 (2014) 598432:1–598432:15.
- [23] E. R. Benton, G. W. Platzman, A table of solutions of the one-dimensional burgers equation, *Quarterly of Applied Mathematics* 30 (2) (1972) 195–212.
- [24] J. Ramos, Picard's iterative method for nonlinear advection–reaction–diffusion equations, *Applied Mathematics and Computation* 215 (4) (2009) 1526–1536, physics and Computation. doi:<https://doi.org/10.1016/j.amc.2009.07.004>.